Article

Critical Role of CDK5 and Polo-like Kinase 2 in Homeostatic Synaptic Plasticity during Elevated Activity

Daniel P. Seeburg,[1] Monica Feliu-Mojer,[1] Johanna Gaiottino,[1] Daniel T.S. Pak,[2] and Morgan Sheng[1],*

[1]The Picower Institute for Learning and Memory, RIKEN-MIT Neuroscience Research Center, Howard Hughes Medical Institute, Massachusetts Institute of Technology, Cambridge, MA 02139, USA
[2]Department of Pharmacology, Med-Dent C405, Georgetown University, 3900 Reservoir Road NW, Washington, DC 20057, USA
*Correspondence: msheng@mit.edu

SUMMARY

Homeostatic plasticity keeps neuronal spiking output within an optimal range in the face of chronically altered levels of network activity. Little is known about the underlying molecular mechanisms, particularly in response to elevated activity. We report that, in hippocampal neurons experiencing heightened activity, the activity-inducible protein kinase Polo-like kinase 2 (Plk2, also known as SNK) was required for synaptic scaling—a principal mechanism underlying homeostatic plasticity. Synaptic scaling also required CDK5, which acted as a "priming" kinase for the phospho-dependent binding of Plk2 to its substrate SPAR, a postsynaptic RapGAP and scaffolding molecule that is degraded following phosphorylation by Plk2. RNAi knockdown of SPAR weakened synapses, and overexpression of a SPAR mutant resistant to Plk2-dependent degradation prevented synaptic scaling. Thus, priming phosphorylation of the Plk2 binding site in SPAR by CDK5, followed by Plk2 recruitment and SPAR phosphorylation-degradation, constitutes a molecular pathway for neuronal homeostatic plasticity during chronically elevated activity.

INTRODUCTION

Long-term potentiation (LTP) and long-term depression (LTD) are examples of Hebbian-type synaptic plasticity, in which correlated patterns of activity in pre- and postsynaptic neurons lead to long-term changes in the strength of their connections. However, the same mechanisms could also result in runaway excitation or depression of neurons. Homeostatic regulation of synaptic strength, such as "synaptic scaling," is generally invoked to prevent such positive-feedback destabilization. Homeostatic mechanisms provide compensatory negative feedback through modulation of global synaptic efficacy and membrane excitability to ensure that neurons remain within a suitable operating range of spiking activity (Burrone and Murthy, 2003; Davis, 2006; Turrigiano, 2007). Despite the presumed importance of synaptic homeostasis, little is known about the molecular mech-

anisms involved in either sensing perturbations from the neuron's operating range or in executing the negative-feedback control. Some progress has been achieved in understanding the homeostatic response to chronic inactivity (e.g., TTX) (Goddard et al., 2007; Gong et al., 2007; Shepherd et al., 2006; Stellwagen and Malenka, 2006; Thiagarajan et al., 2006, 2002), but almost nothing is known about the mechanisms that mediate the adaptation to chronically elevated activity.

Activity-dependent changes in gene expression are likely to be important for the homeostatic response. Indeed, changes in neuronal activity induced by drug administration (Bui et al., 2006; Hevroni et al., 1998; Nedivi et al., 1993; Qian et al., 1993; Yamagata et al., 1993), genetic manipulation (Guan et al., 2005), or sensory deprivation (Majdan and Shatz, 2006; Tropea et al., 2006) affect transcription of numerous genes in both mammals and flies. One activity-regulated gene is Polo-like kinase 2 (*plk2*; also known as serum-inducible kinase [*snk*]), a member of the polo family of serine/threonine protein kinases (Kauselmann et al., 1999; Ma et al., 2003b; Simmons et al., 1992). Polo-like kinases (Plks) contain a C-terminal Polo-box domain (PBD) that mediates autoinhibition of kinase activity as well as phosphorylation-dependent binding to substrates and docking proteins (Elia et al., 2003b; Lowery et al., 2004). Although the closely related kinases Plk1 and Plk3 are critical regulators of the cell cycle (for review, see van de Weerdt and Medema, 2006), Plk2 seems to have a limited role in cell division (Ma et al., 2003a). On the other hand, Plk2 mRNA and protein levels are induced in postmitotic neurons by synaptic activity on the timescale of hours (Kauselmann et al., 1999; Pak and Sheng, 2003).

Recently, it was revealed that the PBD acts as a phospho-peptide-binding domain with preference for peptides that contain the consensus sequence [Ser]-[phospho-Ser/phospho-Thr]-[Pro] (Elia et al., 2003a, 2003b). By phosphorylating such S-S/T-P sequences, proline-directed kinases like CDKs (cyclin-dependent kinases) and MAP kinases could act as "priming" kinases to generate PBD-binding sites, thereby recruiting Plks to specific substrates and docking proteins. Indeed, several recent reports have found evidence for such priming kinase activity in the regulation of Plk function in the cell cycle. For example, cdc2/CDK1 acts as priming kinase to promote the interaction of Plk1 with the centrosome protein Cep55 (Fabbro et al., 2005) and the kinetochore-associated protein Bub1 (Qi et al., 2006).

What is the role of Plk2 in neurons? One action seems to be the phosphorylation and degradation of spine associated RapGAP (SPAR), a protein of the postsynaptic density (PSD) that interacts with PSD-95 (Pak and Sheng, 2003; Pak et al., 2001). The physiological function of SPAR is undetermined, but SPAR promotes the growth of dendritic spines, the postsynaptic compartment of excitatory synapses, at least in part by inhibiting postsynaptic Rap signaling (Pak et al., 2001). Plk2 itself seems to be important for the regulation of spines, as its overexpression causes depletion of mature mushroom spines and the overgrowth of thin, filopodia-like spines (Pak and Sheng, 2003).

In this study, we identify a critical role for Plk2 in homeostatic dampening of quantal amplitude ("synaptic scaling"). CDK5 was also required for synaptic scaling and acted as priming kinase for the phospho-dependent binding between Plk2 and its substrate, SPAR, which promoted Plk2-dependent SPAR degradation. RNAi knockdown of SPAR expression weakened synapses, and overexpression of a SPAR mutant resistant to Plk2 degradation prevented synaptic scaling. Thus, priming phosphorylation of SPAR by CDK5 and subsequent degradation of SPAR by activity-induced Plk2 is an important mechanism of homeostatic plasticity in response to elevated activity.

RESULTS

Plk2 Is Required for Synaptic Scaling and Sufficient to Weaken Synapses

Plk2 protein is induced over a time course of hours during periods of high activity in neurons (Kauselmann et al., 1999; Pak and Sheng, 2003). To investigate the functional significance of Plk2, we made a dominant interfering construct consisting of the C-terminal Plk2-PBD fused to GFP. Because the PBD is critical for proper targeting and functioning of Plks during the cell cycle (Lowery et al., 2004), the Plk2-PBD overexpressed in neurons should block endogenous Plk2 function by competing for PBD-binding sites on Plk2 targets and substrates. Plk1-PBD and Plk3-PBD constructs have been used to dominantly interfere with endogenous Plk1 and Plk3 function (Jiang et al., 2006; Seong et al., 2002).

We transfected GFP-tagged Plk2-PBD ("GFP-PBD") into cultured hippocampal neurons at 16–19 days in vitro (DIV16–19) and analyzed the effects on AMPA receptor (AMPAR)-mediated miniature excitatory postsynaptic currents (mEPSCs; measured in the presence of TTX) 3 days later. To increase network activity and induce endogenous Plk2 expression, cultures were treated for 48 hr with the $GABA_A$ receptor antagonist picrotoxin (PTX, 100 μM), which causes robust induction of Plk2 expression (Pak and Sheng, 2003). In mock-treated cultures, GFP-PBD overexpression had no significant effect on mEPSC amplitude relative to untransfected or GFP-transfected cells (compare "vehicle" in Figures 1A–1F, summarized in 1G and 1H)—perhaps not surprising given that Plk2 is expressed at low levels in unstimulated cultures (Pak and Sheng, 2003). In untransfected and GFP-transfected cells, treatment with PTX resulted in a broad shift in the cumulative distribution of mEPSC amplitudes toward lower values (Figures 1A–1D), consistent with "synaptic scaling" (Turrigiano, 2007; Turrigiano et al., 1998). This leftward shift toward smaller mEPSC amplitudes was prevented in

GFP-PBD-transfected cells; the latter cells actually exhibited a shift toward larger mEPSCs when treated with PTX (Figures 1E and 1F). Average mEPSC amplitude was significantly reduced by PTX in untransfected and GFP-transfected cells, but not in neurons transfected with the dominant-negative GFP-PBD construct (Figure 1G). These results indicate that Plk2 is required for downward scaling of mEPSC amplitude during chronically elevated activity.

We next used a plasmid (pSUPER)-based RNA interference (RNAi) construct (Brummelkamp et al., 2002) to suppress expression of endogenous Plk2 (see Figure S1 available online and Figures 1I and 1J). Following treatment with PTX (48 hr), hippocampal neurons transfected with a control hairpin (scrambled sequence) for 3–4 days showed a decrease in mean mEPSC amplitude comparable in degree to untransfected cells and consistent with synaptic scaling (Figure 1K). RNAi knockdown of Plk2, however, prevented the reduction of mEPSC amplitude after 48 hr PTX (Figures 1I–1K). Similar to GFP-PBD, Plk2 RNAi did not affect basal mEPSC size in the absence of PTX treatment (Figure 1K). The RNAi results corroborate the dominant-negative GFP-PBD findings, showing that Plk2 is required for synaptic scaling of quantal amplitude in response to elevated activity.

In untransfected neurons and in neurons transfected with scrambled RNAi construct or GFP, there was a trend toward decreased mEPSC frequency following 48 hr PTX treatment, but this did not reach statistical significance (Figure 1L). Neither GFP-PBD nor Plk2 RNAi significantly affected mEPSC frequency in basal or PTX conditions relative to untransfected cells (Figure 1L). For these manipulations and those described below, whole-cell capacitances, series resistances, holding currents, mEPSC rise times, and membrane resistances were similar between conditions (Table S1).

We also recorded mEPSCs from cells infected at low titer with Sindbis virus driving expression of wild-type Plk2 (Figures 1M–1O). Compared to control GFP-infected cells, neurons infected with Plk2 and GFP showed a significant drop in mEPSC amplitude. Thus, overexpression of Plk2 is sufficient to weaken synapses.

Phospho-Dependent Binding of Plk2 to SPAR

Precise regulation of subcellular localization is an important mechanism for controlling Plk1 function during cell division (van de Weerdt and Medema, 2006). How might Plk2 be recruited to key target proteins during synaptic homeostasis and how is this recruitment regulated? Plk2 binds via its PBD to the Act2 domain of SPAR, a PSD-95-binding RapGAP enriched in PSDs and dendritic spines (Pak and Sheng, 2003; Pak et al., 2001). Thus, the interaction of Plk2 and SPAR could be one mechanism for targeting Plk2 to postsynaptic sites in neurons. The consensus binding sequence of the PBD contains the core motif -S-S/T-P-, where the central serine or threonine is phosphorylated (Elia et al., 2003b). The -S-S/T-P- sequence is found three times in the Act2 domain of SPAR, with a central serine located at positions 1328, 1384, and 1422 (Figure 2A). Alanine substitution of ser-1328 or the neighboring ser-1327 eliminated interaction between the SPAR-Act2 domain and Plk2-PBD, as measured in yeast two-hybrid assays. Alanine substitution of ser-1383 or ser-1421 had no effect in the same assay (Figure 2B). Conversely, a single-point
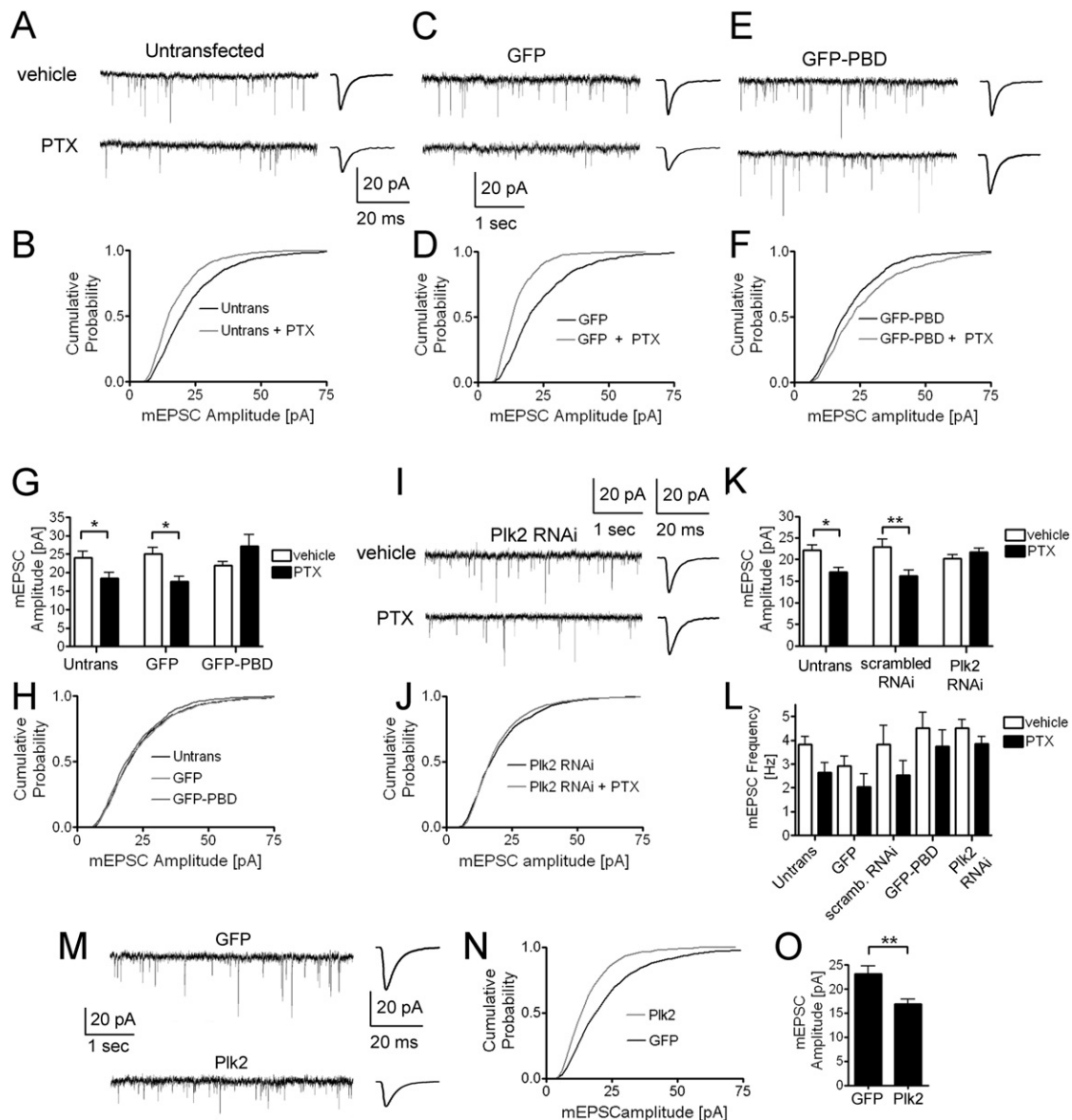
Figure 1. Plk2 Is Required for Synaptic Scaling during Increased Network Activity and Is Sufficient to Dampen Synaptic Strength

(A–F) Sample traces and cumulative distributions. Representative 5 s long sample traces and average mEPSC event traces were taken from individual untransfected cells or cells transfected with GFP or GFP-PBD and treated with either vehicle (DMSO) or PTX (100 μM) for 48 hr, as indicated. Cumulative distribution plots were assembled from the first 100 events from each cell recorded (number of cells as in [G]); $p < 0.001$ (B, D, and F), Kolmogorov-Smirnov test.

(G) Quantification of mean mEPSC amplitude (mean ± SEM) from (A)–(F). n = 10 cells per condition, $*p < 0.05$, Mann Whitney test.

(H) Cumulative distribution of mEPSC amplitudes from neurons that were untransfected or transfected with GFP or GFP-PBD and treated with vehicle; $p > 0.05$, Kolmogorov-Smirnov test.

(I and J) Sample traces and cumulative distribution of mEPSC amplitude from cells transfected with Plk2 RNAi; $p > 0.05$, Kolmogorov-Smirnov test.

(K) Quantification of mEPSC amplitude (mean ± SEM) from RNAi-transfected neurons. n = 9–11 cells per condition, $*p < 0.05$, $**p < 0.01$, Mann Whitney test.

(L) Quantification of mEPSC frequency (mean ± SEM) from neurons transfected as indicated. Neither PTX treatment nor transfection has a significant effect on minifrequency, one-way ANOVA.

(M–O) Sample traces, cumulative distribution, and quantification of mEPSC amplitude (mean ± SEM) from cells infected at low titer (∼50–100 cells infected/15 mm coverslip) with sindbis virus driving expression of either GFP ("GFP") or GFP + Plk2 ("Plk2"). mEPSC recordings were performed ∼24 hr after infection. n = 14 cells per condition, $**p < 0.01$, Mann Whitney test; $p < 0.001$, Kolmogorov-Smirnov test.

mutation at trp-504 of Plk2, a highly conserved residue of the PBD critical for association with Plk-binding sites (Elia et al., 2003b), abolished binding to SPAR-Act2 (Figure 2B). None of these Act2 mutations affected binding of the SPAR-Act2 domain to α-actinin2, another binding partner of SPAR (D.P.S. and D.T.S.P., unpublished data) (Figure 2B).
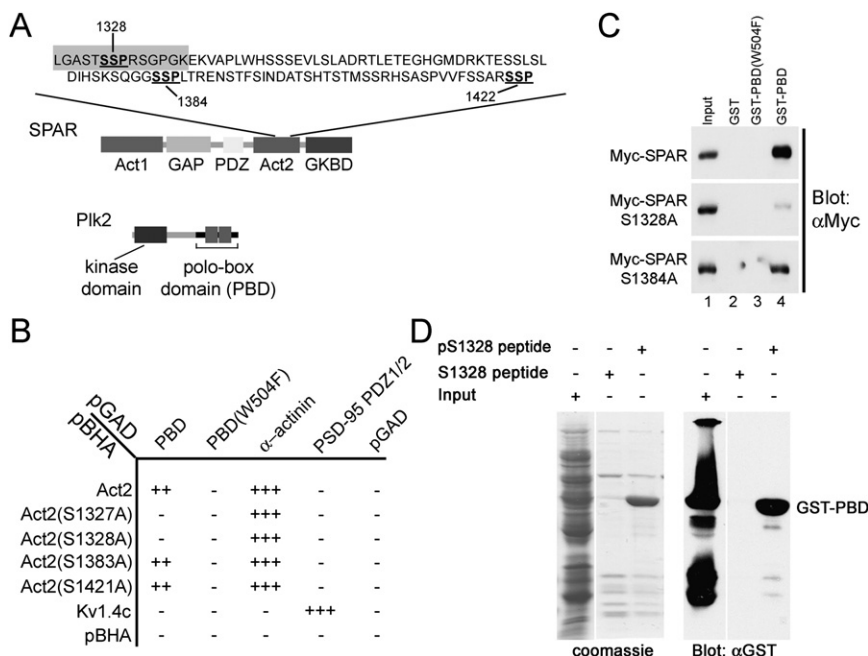
Figure 2. Plk2-PBD Binds to Canonical PBD Binding Site in SPAR

(A) Domain organization of Plk2 and SPAR proteins. Candidate Plk2-PBD-binding sites (SSP) within Act2 domain of SPAR are underlined. pS1328 and S1328 peptide sequences used in (D) are highlighted in gray.

(B) Interaction of the Plk2-PBD (PBD) with SPAR-Act2 and Act2 mutants in yeast two-hybrid system. α-actinin, PSD-95, and Kv1.4 are positive controls. pGAD and pBHA are empty vector negative controls.

(C) Glutathione S-transferase (GST)-PBD pull-down of myc-tagged SPAR and myc-tagged SPAR mutants. Extracts of HEK293 cells transfected with myc-tagged SPAR or indicated SPAR mutants were incubated with glutathione Sepharose beads coupled to GST alone, GST-PBD(W504F), or GST-PBD, as indicated. Bound proteins were immunoblotted for myc. Lane 1 was loaded with 0.5% of the input.

(D) Binding of GST-PBD to phosphorylated ser-1328 peptide (pS1328). pS1328 and nonphosphorylated S1328 peptides were coupled to agarose beads and incubated with extracts from bacteria expressing GST-PBD. Bound proteins were analyzed by Coomassie blue staining or immunoblotting with GST antibodies. Input lane, 10% of extract loaded onto beads.

In "pull-down" experiments, a GST fusion protein of Plk2′s PBD (GST-PBD) precipitated full-length wild-type SPAR expressed in HEK293 cells, but not mutant SPAR in which ser-1328 was changed to alanine [SPAR(S1328A)] (Figure 2C, lane 4). GST-PBD also precipitated full-length SPAR(S1384A) (lane4), while GST and GST-PBD(W504F) failed to pull down any of the SPAR constructs (Figure 2C, lanes 2–3). Thus, the -S-S-P- motif centered on ser-1328 of SPAR is necessary for full-length SPAR to bind to the PBD of Plk2.

We tested whether the Plk2-PBD interaction with SPAR requires phosphorylation of ser-1328. In pull-down experiments, a nonphosphorylated peptide comprising amino acids 1322–1335 of SPAR ("S1328 peptide," highlighted in gray in Figure 2A) coupled to agarose beads failed to precipitate GST-PBD expressed in bacteria (Figure 2D). The same peptide phosphorylated on ser-1328 ("pS1328 peptide") efficiently pulled down the PBD fusion protein (Figure 2D). Thus, the PBD of Plk2 binds specifically to a peptide motif in SPAR centered on ser-1328, and only when ser-1328 is phosphorylated.

Phosphorylation of Serine 1328 Is Important for Plk2-Mediated Degradation of SPAR

Overexpression of Plk2 and SPAR in heterologous cells results in Plk2-mediated phosphorylation and degradation of SPAR (Pak and Sheng, 2003). Here, we used a tetracycline-inducible ("Tet On") promoter system to turn on the expression of Plk2 in HEK293 cells also expressing SPAR from a constitutive promoter. Following application of doxycycline (100 ng/ml), wild-type SPAR was lost over the course of a few hours (presumably degraded) with rising expression of wild-type Plk2 (Figure 3A, quantified in 3B). Induction of a kinase-dead mutant of Plk2 [K.D. Plk2(K108M)] failed to cause degradation of SPAR (Figures

3A and 3B). Mutations in the PBD of Plk2 at either trp-504 [Plk2(W504F)] or at his-626 and lys-628 [Plk2(H626A K628M)] (two residues responsible for phospho-dependent binding of the PBD [Elia et al., 2003b]), also prevented degradation of SPAR by Plk2. Most importantly, the SPAR mutant defective in PBD binding [SPAR(S1328A)] was poorly degraded by wild-type Plk2 (Figures 3A and 3B). Thus, ser-1328 of SPAR and an intact PBD of Plk2 are critical for Plk2-mediated degradation of SPAR, most likely because interaction of the PBD with phosphorylated ser-1328 is required for Plk2 recruitment to this target.

CDK5 Is a 'Priming' Kinase for SPAR ser-1328

To study more directly SPAR phosphorylation on ser-1328, we raised phospho-specific antibodies against the pS1328 phosphopeptide (see Figure 2A). The affinity-purified antibody ("α-pS1328SPAR") recognized the phosphorylated S1328 peptide on slot blots, but not the unphosphorylated peptide (Figure 4A). On western blots, α-pS1328SPAR detected a signal from wild-type myc-tagged SPAR expressed in HEK293 cells, but not myc-SPAR(S1328A) (Figure 4B, compare lanes 1–6 with lanes 7–12). Collectively, these data indicate that α-pS1328SPAR specifically recognizes SPAR phosphorylated on ser-1328.

Because ser-1328 precedes a proline residue (-S-S^{1328}-P-R-S-), we supposed that a proline-directed kinase is responsible for phosphorylating this residue in SPAR. We tested drug inhibitors of several proline-directed kinases by applying them to HEK293 cells overexpressing myc-tagged SPAR. Inhibitors of the MAP kinases p38 (SB-202190, 5 μM), JNK (SP-600125, 20 μM), or Erk, through its upstream activator MEK (PD-98059, 50 μM), had no effect on ser-1328 phosphorylation of SPAR, as measured by immunoblotting with α-pS1328SPAR (Figure 4C, quantified in 4D). Roscovitine (10 μM), a CDK5 inhibitor that can
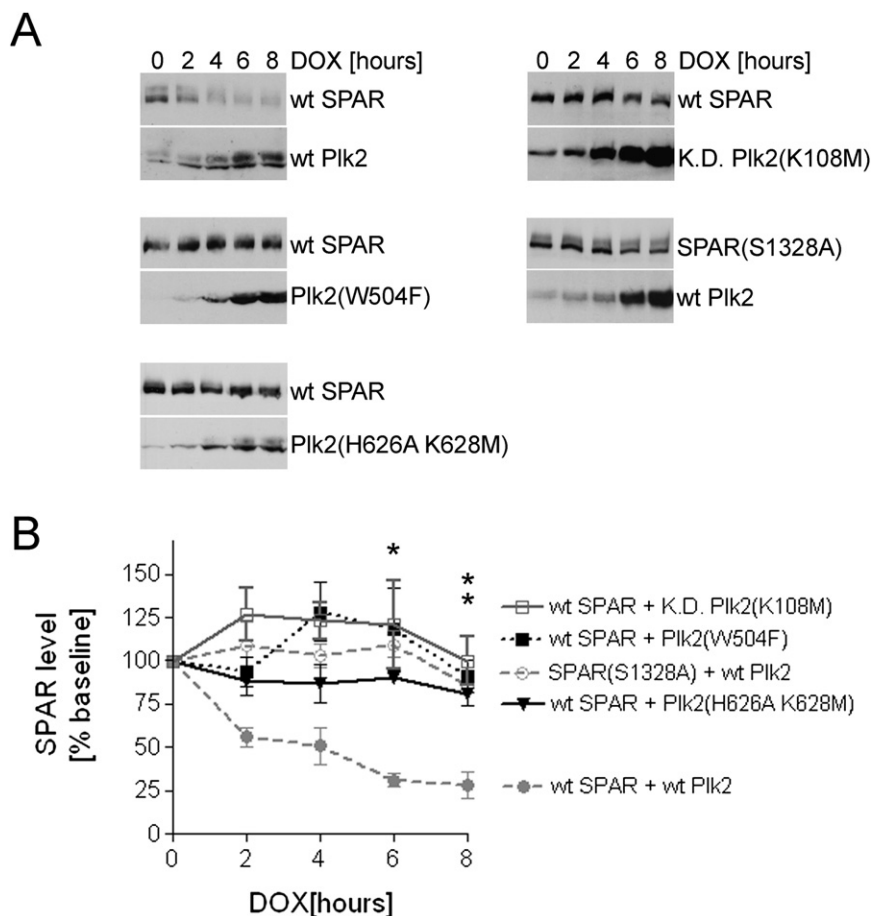
A

B

also block CDK1 and CDK2 at this concentration (Meijer et al., 1997), significantly decreased the α-pS1328SPAR signal (Figures 4C and 4D).

To test whether neuron-specific CDK5 can phosphorylate ser-1328 of SPAR, we coexpressed SPAR with CDK5 and its activator p35 in HEK293 cells; ser-1328 phosphorylation was strongly enhanced (Figure 4B, lane 3; quantified in 4D). No effect on SPAR ser-1328 phosphorylation was observed with a kinase-dead CDK5 construct ("CDK5-DN," carrying an asp-144-to-asn mutation [Nikolic et al., 1996]) or with constitutively active forms of JNK1 or MEK1 (an upstream activator of Erk) (Figure 4B, quantified in 4D). KN-93 (5 μM), an inhibitor of CaMKII, had no effect on ser-1328 phosphorylation (Figures 4C and 4D). These results are consistent with motif predictions (Scansite) (Obenauer et al., 2003), in which the sequence surrounding ser-1328 scored highest as a CDK5 phosphorylation motif.

Is endogenous SPAR phosphorylated on ser-1328 in neurons? On immunoblots of rat hippocampal extracts, α-pS1328SPAR detected a band of molecular weight similar to that of recombinant SPAR (Figure 5A, where "R" denotes lanes loaded with recombinant SPAR expressed in HEK293 cells). This band was "quenched" by competition with excess of the phospho-S1328 peptide, but not the unphosphorylated peptide (Figure 5A, lanes 4 and 3). In addition, treatment of the membranes with calf intestinal phosphatase (CIP) eliminated the

α-pS1328SPAR signal, while the signal from a C-terminal SPAR antibody persisted (Figure 5A, lanes 7–12). We conclude that α-pS1328SPAR specifically detects phosphorylated SPAR in neurons. Unfortunately, the α-pS1328SPAR phosphoantibodies gave no significant signal by immunocytochemistry of cultured neurons.

SPAR was phosphorylated on ser-1328 in cultured cortical neurons (DIV12), as detected by immunoblotting with α-pS1328SPAR (Figure 5B). As in heterologous cells, the α-pS1328SPAR signal in neurons was reduced by application of the CDK5 inhibitor roscovitine for either 2 hr (data not shown) or for 12–18 hr (Figure 5B, compare lanes 2 and 4 to lanes 1 and 3, respectively). Inhibitors of JNK (SP-600125), MEK (PD-98059), p38 (SB-202190), or CaMKII (KN-93) had no effect on phospho-ser-1328 SPAR levels in neurons (Figure 5B, lanes 5–12).

To test whether endogenous CDK5 activity affects SPAR ser-1328 phosphorylation, we infected cultured cortical neurons with HSV virus driving expression of GFP alone or GFP together with the CDK5 activator p35. Compared with control infection with GFP alone, cortical cultures infected with p35 + GFP showed a significant increase in endogenous SPAR ser-1328 phosphorylation (Figure 5C). Together with the pharmacological data (Figure 5B), these results show that a subpopulation of SPAR is phosphorylated on ser-1328 in neurons and that this phosphorylation is enhanced by CDK5.

CDK5 activity is stimulated by Aβ peptide (Alvarez et al., 2001; Town et al., 2002), a proteolytic product of the amyloid precursor protein (APP) that is implicated in the pathogenesis of Alzheimer's disease (Walsh and Selkoe, 2004). We found that overnight (~15 hr) treatment with soluble Aβ(1-40), but not the reverse peptide Aβ(40-1), elevated the phosphorylation of ser-1328 on
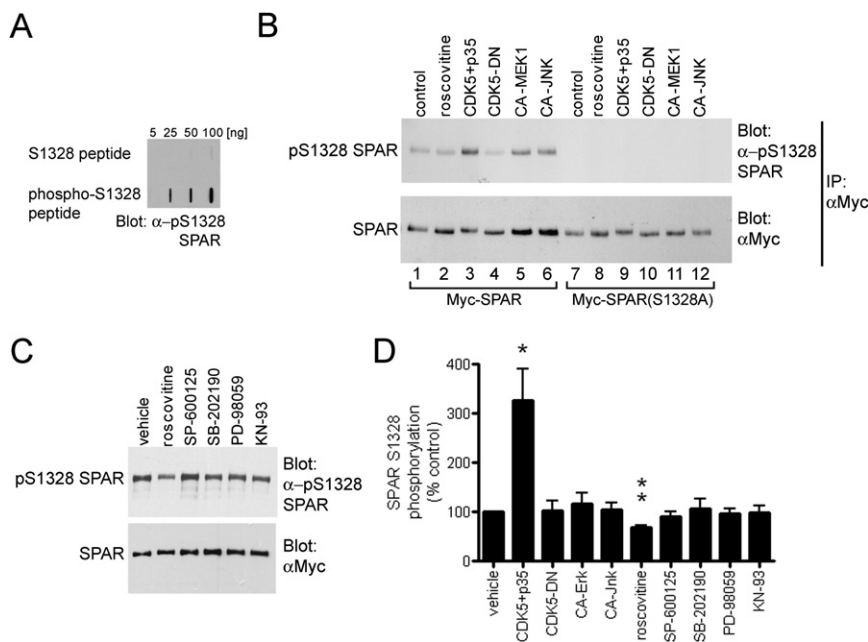
Figure 4. Phosphorylation of SPAR ser-1328 and Regulation by CDK5

(A) "Slot blots" showing specificity of the α-pS1328SPAR phospho-antibody for the phosphorylated S1328 peptide. Peptides were bound to nitrocellulose and immunoblotted with α-pS1328SPAR.

(B) CDK5 enhances ser-1328 phosphorylation in heterologous cells. Myc-tagged wild-type SPAR or SPAR(S1328) was transfected into HEK293 cells with the indicated protein kinase constructs or treated with roscovitine for 2 hr. SPAR was immunoprecipitated with myc antibody and immunoblotted with α-pS1328SPAR followed by stripping and reprobing with myc antibodies.

(C) CDK5 inhibitor roscovitine reduces SPAR ser-1328 phosphorylation. HEK293 cells were transfected with myc-SPAR and treated for 2 hr with the indicated drugs, then immunoblotted with α-pS1328SPAR, stripped, and reprobed with myc antibodies.

(D) Quantification of data from (B) and (C), normalized to control conditions from the same blot (mean ± SEM). n = 5–6 for each condition, except roscovitine (n = 11). *p < 0.05, **p < 0.01, compared to control (100%), two-tailed t test.

SPAR in cortical neurons, consistent with increased activity of CDK5 (Figure S2).

CDK5 Activity Promotes Degradation of SPAR

We showed that the SPAR(S1328A) mutant is protected from degradation by Plk2 in HEK293 cells, presumably because it cannot be phosphorylated at its PBD-binding site and thus cannot interact with the Plk2-PBD (see Figure 3). We tested this hypothesis further by repeating the same SPAR degradation assay in the presence of roscovitine, which reduced basal phosphorylation of SPAR ser-1328 in HEK293 cells (see Figures 4C and 4D). In the absence of roscovitine, doxycycline induced the expression of Plk2 and concomitant degradation of SPAR (Figure 6A). SPAR degradation was impaired by treatment of the cells with roscovitine (Figure 6A). Our results support the idea that CDK5 activity promotes SPAR degradation by "priming" phosphorylation of ser-1328 in the Plk2-PBD-binding site.

Overexpression of Plk2 promotes SPAR degradation in neurons (Pak and Sheng, 2003). Because CDK5 regulates neuronal SPAR ser-1328 phosphorylation (Figures 5B and 5C), we wondered whether CDK5 activity contributes to SPAR degradation in neurons as well. Indeed, cultured hippocampal neurons (DIV21–28) treated with roscovitine for 12–18 hr showed increased endogenous SPAR levels by immunocytochemistry (Figure 6B, quantified in 6C). Interestingly, the enhancement in SPAR staining intensity was greatest in dendritic regions close to the cell body and insignificant in the most distal dendrites (Figure 6C). This proximal-distal gradient is reminiscent of the activity-induced pattern of Plk2 protein expression, which is also highest in proximal dendrites and tapers off with distance from the cell body, and of the graded effect of Plk2 induction on dendritic SPAR levels (Pak and Sheng, 2003). Our result is thus consistent with CDK5 stimulating the degradation of SPAR in neurons via a Plk2-dependent mechanism.

To corroborate the pharmacological data, we transfected DIV16 hippocampal neurons for 3 days with a GFP-tagged dominant-negative CDK5 construct (GFP-CDK5-DN). Overexpression of GFP-CDK5-DN, but not wild-type GFP-CDK5, increased SPAR immunostaining intensity relative to control cultures transfected with GFP alone (Figure 6D, quantified in 6E). These results imply that CDK5 activity promotes the loss of SPAR, thus supporting the idea that endogenous CDK5 acts as a priming kinase for the degradation of SPAR.

CDK5 and SPAR Participate in Homeostatic Plasticity

If CDK5 priming activity is important for Plk2-dependent functions like degradation of SPAR, blocking CDK5 activity might also interfere with synaptic scaling, which requires Plk2. We therefore tested the effect of the dominant-negative CDK5 construct (CDK5-DN) on mEPSCs. As expected, in untransfected cells, 48 hr of PTX treatment caused a significant shift in the cumulative distribution of mEPSC amplitudes toward smaller values, as well as a significant drop in the mean mEPSC amplitude, reflecting normal synaptic scaling (Figure 7A). Overexpression of CDK5-DN had a small nonsignificant effect on mean mEPSC amplitude in the absence of PTX treatment, but it prevented the reduction in mEPSC amplitude induced by PTX (Figure 7A). These results show that CDK5 is required under conditions of elevated activity for dampening synaptic strength and thus for homeostatic plasticity. The effect of CDK5-DN is similar to that of dominant-negative GFP-PBD and Plk2 RNAi (see Figure 1), consistent with the idea that CDK5 and Plk2 act in the same pathway to mediate synaptic homeostasis. Further supporting this notion, cells transfected with both CDK5-DN and GFP-PBD showed a similar degree of disruption of synaptic scaling as cells transfected with either construct alone (Figure 7A). CDK5-DN had no effect on mEPSC frequency compared to untransfected cells (data not shown).
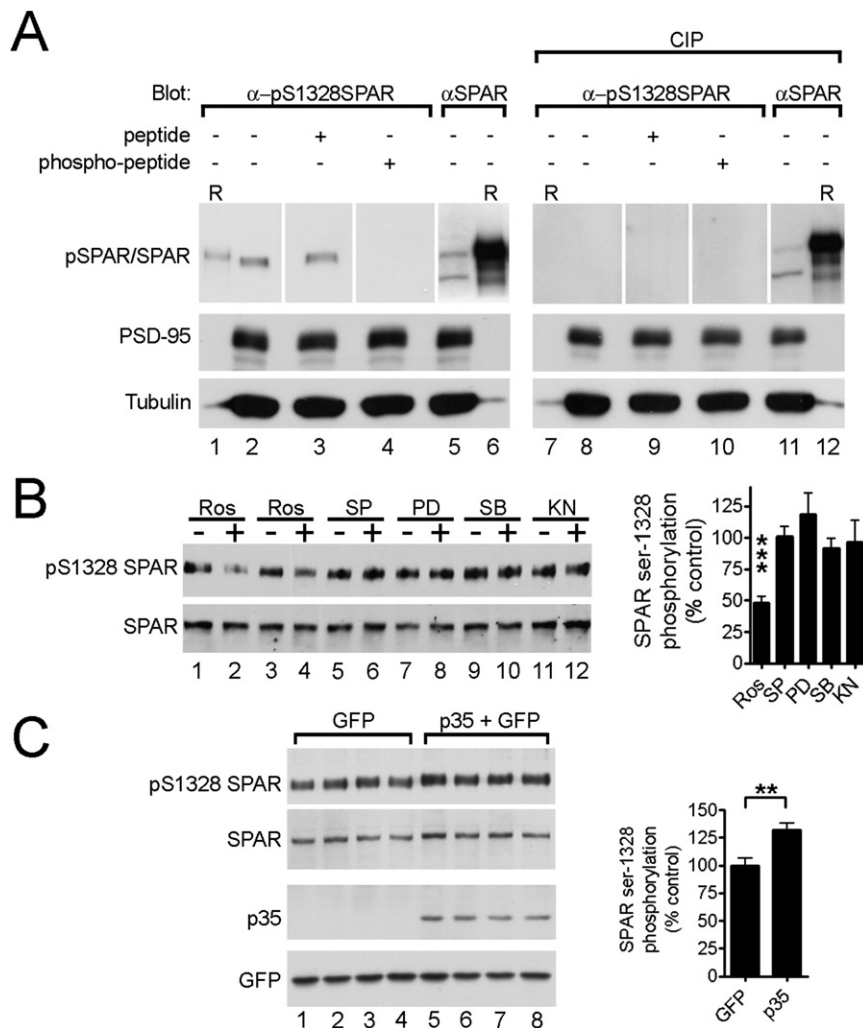
Figure 5. Regulation of SPAR ser-1328 Phosphorylation in Neurons

(A) Phosphorylation of SPAR ser-1328 in rat hippocampus. Total hippocampal extracts were immunoblotted with either α-pS1328SPAR or SPAR antibodies (upper row) and with PSD-95 or tubulin antibodies, as indicated. The pS1328SPAR signal was specifically eliminated by competition with the phospho-S1328 peptide (lane 4), but not by the unphosphorylated S1328 peptide (lane 3). Calf intestinal phosphatase (CIP) treatment of the membrane eliminated the pS1328SPAR signal (lanes 7–10). "R" lanes were loaded with HEK293 cell extract expressing recombinant SPAR protein.

(B) Ser-1328 SPAR phosphorylation in neurons reduced by CDK5 inhibitor. Dissociated high-density cortical cultures (DIV12) were treated for 12–18 hr with vehicle (DMSO) or roscovitine ("Ros," 10 μM), SP-600125 ("SP," 20 μM), PD-98059 ("PD," 50 μM), SB-202190 ("SB," 5 μM), or KN-93 ("KN," 5 μM). Total cell lysates were immunoblotted with α-pS1328SPAR, then stripped and reprobed with SPAR antibodies (left). Bar graph (right) shows quantification of blots, normalized to control conditions from the same blot (mean ± SEM). n = 7–9 for each condition. ***$p < 0.001$, compared to control (100%), two-tailed t test.

(C) Regulation of ser-1328 SPAR phosphorylation in neurons by CDK5. High-density cortical (DIV12) cultures were infected for ~24 hr with HSV driving expression of either GFP alone (lanes 1–4) or GFP together with the CDK5 activator p35 (lanes 5–8). Total cell lysates were immunoblotted with the indicated antibodies (left) and quantified (mean ± SEM, normalized to control GFP-infected cells) (right). n = 16 for each condition, **$p < 0.01$, Mann Whitney test.

Does Plk2 dampen synaptic strength during homeostatic plasticity through degradation of SPAR? To address this question, we transfected cells with either WT SPAR or SPAR(S1328A), which carries a mutation in the Plk2-binding site and is resistant to degradation by Plk2 (see Figure 3). Neurons transfected with either WT SPAR or SPAR(S1328A) showed a trend toward increased mean mEPSC amplitude relative to untransfected cells, but this effect did not reach statistical significance (Figure 7B). mEPSC frequency was also unchanged in neurons transfected with either WT SPAR or SPAR(S1328A) (data not shown). In untransfected cells and cells transfected with WT SPAR, 48 hr of PTX treatment caused a significant drop in mEPSC amplitude (Figure 7B), consistent with normal homeostatic plasticity. In contrast, cells transfected with SPAR(S1328A) failed to undergo synaptic scaling in response to PTX treatment (Figure 7B). These results thus link degradation of SPAR to Plk2-mediated synaptic weakening during chronically elevated activity.

If Plk2-mediated degradation of SPAR contributes to downscaling of mEPSCs during elevated activity, knockdown of SPAR expression by RNAi might mimic that effect. Indeed, cells transfected with an RNAi construct targeting endogenous SPAR showed significantly diminished mEPSC amplitude compared to untransfected cells and cells transfected with a control RNAi construct against firefly luciferase ("FF RNAi") (Figure 7C). Together with the finding of impaired homeostasis in neurons expressing SPAR(S1328A), these data suggest that activity-dependent depletion of SPAR is an important mechanism for synaptic weakening during homeostatic plasticity. A molecular model of activity-dependent synaptic scaling based on these results is shown in Figure 8.

DISCUSSION

Activity-Inducible Plk2 and Synaptic Scaling

Homeostatic plasticity has emerged as an important regulatory mechanism for stabilizing the activity of neurons and circuits. Among its proposed functions are prevention of epilepsy, balancing of excitation and inhibition, stabilization of neurons during Hebbian plasticity, and regulation of spontaneous network activity during development (Davis, 2006; Gonzalez-Islas and Wenner, 2006; Turrigiano, 2007).
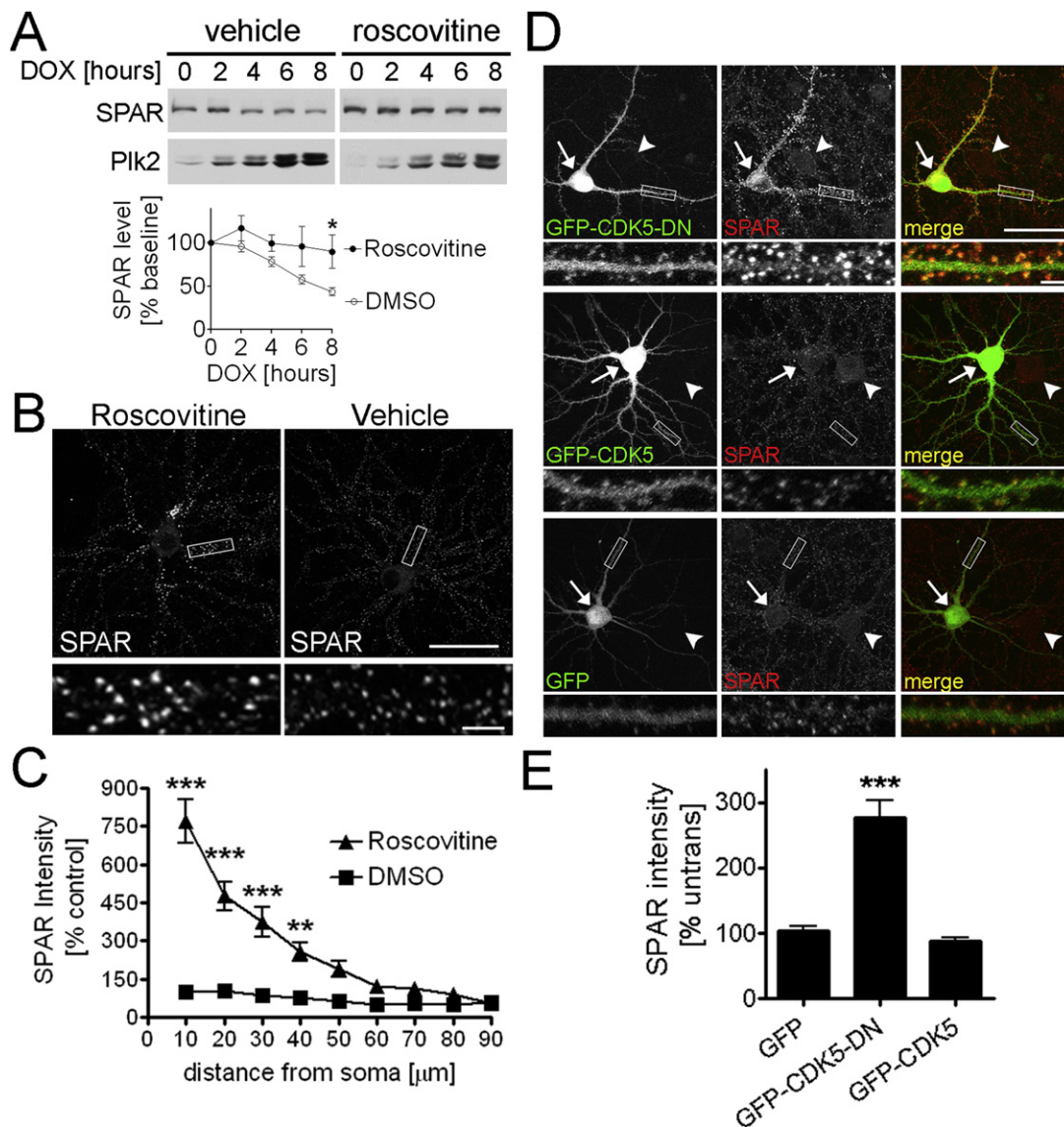
Figure 6. CDK5 Promotes Degradation of SPAR

(A) Roscovitine prevents SPAR degradation by Plk2 in heterologous cells. HEK293 cells triple transfected with myc-tagged WT SPAR, tet-inducible myc-tagged WT Plk2, and the pTET-On vector were immunoblotted (top) with myc antibodies after doxycycline treatment (as in Figure 3). HEK293 cells were treated with either DMSO ("vehicle") or roscovitine (10 μM), as indicated, for the final 8 hr before lysis. SPAR levels were quantified (mean ± SEM) and plotted as a function of DOX induction time for DMSO and roscovitine treatment conditions (bottom). n = 5 (DMSO), n = 9 (roscovitine). *p < 0.05, curves are different, two-way ANOVA.

(B) Increased SPAR immunostaining in neurons following pharmacological inhibition of CDK5. Example of hippocampal neurons (DIV21–28) treated for 12–18 hr with either roscovitine (10 μM) or vehicle (DMSO) and stained with SPAR antibodies to visualize endogenous SPAR protein. The boxed region is shown at higher magnification below. Scale bar: 50 μm low magnification and 5 μm high magnification.

(C) Quantification of dendritic SPAR immunofluorescence intensity data from (B), plotted as a function of distance from the cell body (see Experimental Procedures) (mean ± SEM). SPAR immunofluorescence intensity from both treatment conditions was normalized to the 10 μm distance of DMSO-treated neurons. n = 18 cells (roscovitine), n = 16 cells (DMSO), **p < 0.01, ***p < 0.001, two-way ANOVA with post test.

(D) SPAR accumulation in neurons overexpressing dominant-negative CDK5 (GFP-CDK5-DN). DIV16 hippocampal neurons were transfected with GFP-tagged CDK5(D144N) ("GFP-CDK5-DN"), WT GFP-CDK5, or GFP, fixed at DIV19, and stained with SPAR antibodies to visualize endogenous SPAR protein. The merge of the two signals is shown in color. Scale bar: 50 μm (low magnification) and 5 μm (high magnification).

(E) Quantification of SPAR immunofluorescence intensity data from (D). Histograms (mean ± SEM) are normalized to neighboring untransfected neurons. n = 16 cells (all constructs), ***p < 0.001, GFP-CDK5-DN is significantly different than other conditions, one-way ANOVA.

A few reports have addressed molecular mechanisms that contribute to homeostasis following chronic reduction of neuronal activity. Release of TNF-α from glia (Stellwagen and Malenka, 2006), regulation of the β to αCaMKII ratio (Thiagarajan et al., 2002), BDNF (Rutherford et al., 1998), adenylyl cyclase 1 (Gong et al., 2007), and downregulation of the activity-inducible
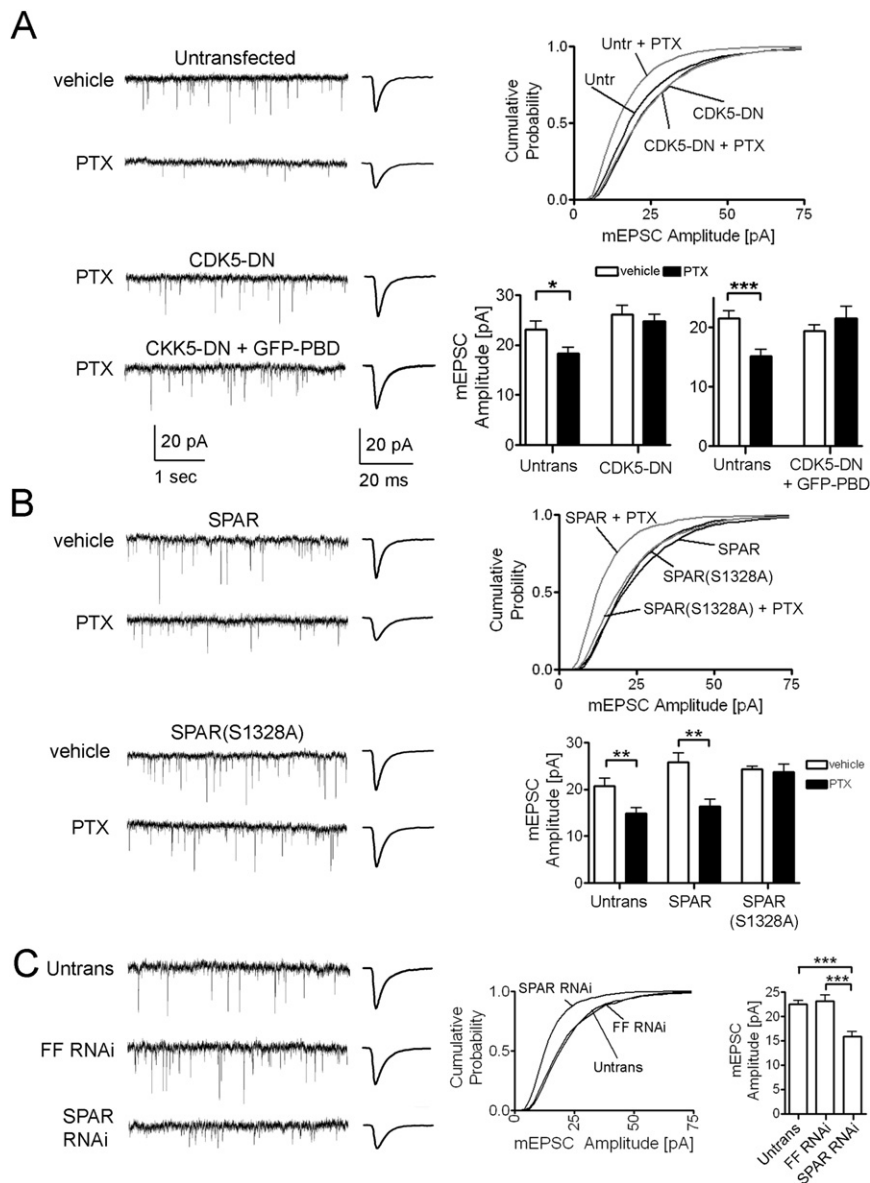
Figure 7. CDK5 and SPAR Participate in Homeostatic Plasticity

(A) CDK5 inhibitor impairs synaptic homeostasis during heightened activity. Representative 5 s sample traces and average mEPSC event traces from individual untransfected cells and cells transfected with either GFP-tagged CDK5(D144N) ("CDK5-DN"), or CDK5-DN together with GFP-PBD ("CDK5-DN + GFP-PBD"), treated with either vehicle (DMSO) or PTX for 48 hr, as indicated (left). Cumulative distributions (top right) of mEPSC amplitudes were generated from the first 100 events of recorded cells from conditions as indicated. "Untr" is significantly different than "Untr + PTX" and "CDK5-DN," p < 0.001; "CDK5-DN" is not significantly different than "CDK5-DN + PTX," p > 0.05; Kolmogorov-Smirnov test. Bar graphs (bottom right) show quantitation of mEPSC amplitude (mean ± SEM). n = 17–19 cells per condition (left bar graph); n = 11–16 cells per condition (right bar graph); *p < 0.05, ***p < 0.001, Mann Whitney test.
(B) SPAR mutant resistant to Plk2 degradation prevents synaptic scaling. Sample traces (left), cumulative distributions (top right), and quantification of mEPSC amplitude (mean ± SEM; bottom right) from neurons transfected with wild-type SPAR or SPAR(S1328A), and treated with PTX, as indicated, **p < 0.01, Mann Whitney test. Cumulative distribution of "SPAR" is significantly different than "SPAR + PTX," p < 0.001; "SPAR(S1328A)" is significantly different than "SPAR(S1328A) + PTX," p < 0.01; Kolmogorov-Smirnov test. n = 12–14 cells per condition.
(C) RNAi knockdown of SPAR weakens synapses. Representative mEPSC traces from untransfected cells and cells transfected with SPAR RNAi or negative control firefly luciferase RNAi ("FF RNAi") (left). Cumulative distribution plot (middle) and bar graphs of mEPSC amplitude (mean ± SEM; right) quantify the effect of SPAR RNAi knockdown. Cumulative distribution of "SPAR RNAi" is significantly different than "Untrans" and "FF RNAi," p < 0.001; "FF RNAi" is not significantly different than "Untrans," p > 0.05; Kolmogorov-Smirnov test. n = 11–15 cells per condition, ***p < 0.001, Mann Whitney test.

gene *arc/arg3.1* (Shepherd et al., 2006) were shown to be important for the upregulation of mEPSC amplitude and/or frequency following prolonged inactivity in cultured neurons. Hippocampal cultures from *arc/arg3.1* knockout mice continued to display significant downscaling of mEPSCs in response to chronic hyperactivity induced by the GABA_A blocker bicuculline, leading the authors to conclude that mechanisms apart from Arc/Arg3.1 are likely to be important for the weakening of synapses following long-term increases in activity (Shepherd et al., 2006). Our study points to Plk2 in this role.

Key questions in homeostatic plasticity include the following. What are the molecules involved in sensing perturbations from a set point? And how are these transduced into a negative-feedback response appropriate for the type and magnitude of the initial perturbation? Postsynaptic calcium levels are positively correlated with neuronal activity (Goldberg and Yuste, 2005; Ross,

1989), and calcium sits atop numerous biochemical signaling cascades affecting gene expression (Burgoyne et al., 2004). The induction of Plk2 protein by activity takes many hours and involves calcium entry through voltage-gated calcium channels and/or NMDA receptors, as well as activation of the calcium-calmodulin-dependent protein phosphatase PP2B/calcineurin (Pak and Sheng, 2003). Thus, intracellular calcium elevation and a delayed rise in Plk2 expression provide a means of sensing prolonged increases in ambient network activity. Because it phosphorylates key substrate(s) that regulate synapse morphology and function, the Plk2 protein kinase can then transduce the elevated activity into a negative-feedback response that dampens synaptic strength. Thus, Plk2 provides a link between sensing elevated activity and the homeostatic feedback response.

Our findings point to the degradation of SPAR as an important mechanism of Plk2-mediated weakening of synapses. RNAi
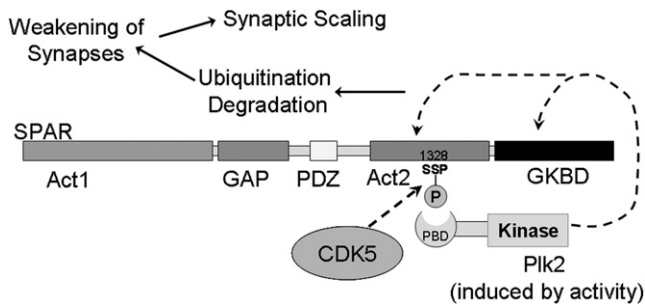
Figure 8. Model for Plk2-Dependent Synaptic Scaling
Priming phosphorylation of SPAR ser-1328 by CDK5 recruits activity-induced Plk2 to SPAR, followed by phosphorylation of SPAR by Plk2, ubiquitination-degradation of SPAR, and synaptic weakening.

experiments show that loss of SPAR depresses synaptic strength; more significantly, synaptic homeostasis is disrupted when a SPAR mutant resistant to Plk2-mediated degradation is overexpressed in neurons. Degradation of the postsynaptic RapGAP SPAR by Plk2 would be expected to enhance the activity of postsynaptic Rap GTPases, which are known to depress synaptic transmission (Huang et al., 2004; Zhu et al., 2002, 2005) and cause thinning of spines (Fu et al., 2007; Xie et al., 2005). In addition to effects on Rap signaling, SPAR may also promote spine morphogenesis and synaptic function via its scaffolding or actin-binding properties (Pak et al., 2001).

CDK5 Priming and Regulation of Plk2 Function
Degradation of SPAR by Plk2 requires phosphorylation of SPAR on ser-1328. We identify CDK5 as the likely proline-directed kinase that "primes" this site, generating a phosphomotif that is specifically recognized by the PBD of Plk2. Inhibition of CDK5 led to decreased ser-1328 phosphorylation and increased SPAR protein levels in neurons. More importantly, CDK5 activity was required for suppression of mEPSC amplitude during elevated network activity. These results are consistent with CDK5 playing a critical role in synaptic homeostasis.

We further note that ser-1328 lies in SPAR's Act2 domain, which interacts with the actin cytoskeleton (Pak et al., 2001). We speculate that in addition to priming SPAR for phosphorylation and degradation by Plk2, ser-1328 phosphorylation might release SPAR from association with actin. The latter event might facilitate release of SPAR from the PSD and subsequent interaction with Plk2.

The regulation of CDK5 by synaptic activity is poorly understood. Currently, CDK5 activity is believed to be mainly regulated by the abundance of its activator subunits p39 and p35. Treatment with excitotoxic levels of glutamate increases CDK5 activity through calpain-mediated cleavage of p35 to p25 (Lee et al., 2000), whereas lower levels of glutamate ($\leq$0.1 mM) seem to reduce CDK5 activity by proteasomal degradation of p35 (Hosokawa et al., 2006; Wei et al., 2005). It would be interesting to define in more detail the regulation of CDK5 by synaptic activity, because local modulation of CDK5 could impart local priming of SPAR, leading to synapse-specific actions of Plk2.

The amyloid-β peptide (Aβ) can also induce the conversion of p35 to p25 (Lee et al., 2000) and activate CDK5 (Roselli et al.,

2005; Town et al., 2002). Consistent with these studies, we found that prolonged exposure of neurons to Aβ resulted in an increase in SPAR-ser-1328 phosphorylation. Soluble Aβ, which is probably an important toxic mediator in Alzheimer's disease (Mattson, 2004; Walsh and Selkoe, 2004), inhibits synaptic transmission at least in part via endocytic removal of AMPARs (Hsieh et al., 2006; Kamenetz et al., 2003). Our study introduces a mechanism by which Aβ could cause weakening and loss of synapses—namely, increased phosphorylation of SPAR by CDK5, priming SPAR for degradation by Plk2 during periods of heightened activity.

The fact that CDK5 phosphorylation generates a Polo-box-binding site in SPAR raises the intriguing possibility that Plk2 function in neurons can be controlled by the regulated recruitment of Plk2 to phosphorylated -S-S/T-P- motifs on SPAR and other targets. Plk2 function would then require the coincidence of two conditions—prolonged elevated neuronal activity to induce Plk2 protein expression as well as the availability of primed binding sites for the PBD—thus allowing for spatial and temporal refinement in the control of Plk2 activity.

In the cell cycle, priming kinases like cdc2/CDK1 regulate the availability of Plk-binding sites to ensure that the many functions of mitotic Plks are carried out with required precision in time and subcellular location (van de Weerdt and Medema, 2006). Similarly, precise regulation in neurons might allow the specific recruitment of Plk2 to synapses that have been "tagged" by the phosphorylation of SPAR ser-1328 or other PBD-binding sites. Such synapse-specific tagging of target proteins could arise from localized activation of CDK5 (or other priming kinases), though this remains to be shown for CDK5. In this context, it is noteworthy that Plk2 protein levels are higher in proximal than in distal dendrites after 18–24 hr of PTX induction (Pak and Sheng, 2003).

How might this proximal-to-distal gradient be reconciled with the view that homeostatic plasticity acts globally in neurons? One possibility is that the gradient seen by Pak and Sheng (2003) forms only during the early phase of induction of Plk2 and is dissipated by 48 hr, when most electrophysiological measurements of synaptic scaling (including our experiments here) are performed. Alternatively, homeostatic synaptic plasticity may not be as global as presumed (see Turrigiano, 2007). Indeed, recent studies have suggested the existence of "local" homeostatic mechanisms occurring at the level of individual dendritic segments (Ju et al., 2004; Sutton et al., 2006) or even individual synapses (Hou et al., 2008). An important role of homeostatic plasticity is the stabilization of neuronal firing rates (Burrone and Murthy, 2003), which would be predicted to be most effective if concentrated on dendritic segments closest to the soma. Thus, there may be a cellular logic to exerting a proximal-to-distally graded mechanism of homeostatic change.

EXPERIMENTAL PROCEDURES

DNA Constructs
GFP-PBD was generated by PCR of the Plk2-PBD (aa 332–682) followed by insertion into a β-actin-driven GFP vector. rtTA-responsive Plk2 was generated by PCR of myc-tagged full-length Plk2 from pGW1, followed by insertion into pTRE (Clontech). For Plk2 RNAi, the following siRNA sequence was cloned into pSUPER (Brummelkamp et al., 2002): 5′-GCATAAGAGAAGCAAGATA-3′. The

scrambled siRNA sequence in pSUPER used was 5′-GAACGAGTGTCTG TAAGTA-3′ and was a gift from Eunjoon Kim (KAIST). Site-directed mutagenesis was performed using "Quickchange" (Stratagene), and all constructs were verified by DNA sequencing. GFP-CDK5, GFP-CDK5-DN, and GFP-p35 were gifts from Li-Huei Tsai. The following constructs have been described: Kv1.4 C terminus in pBHA, and PSD-95 PDZ 1/2 in pGAD10 (Kim et al., 1995), Act2 in pBHA, Plk2-PBD in pGAD, myc-tagged SPAR in pGW1, GST-tagged Plk2-PBD in pGEX (Pak and Sheng, 2003; Pak et al., 2001), α-actinin-2 (A2.10) in pGAD (Wyszynski et al., 1997). siRNA sequences for SPAR (5′-CCGCCTG AAGTCTCTGATTAA-3′) and firefly luciferase (5′-CCGCCTGAAGTCTCTGAT TAA-3′) in pENTR-Mir U6 vectors were gifts from Wade Harper (Harvard).

Antibodies, Aβ(1-40), and Drugs

Phospho-specific α-pS1328 SPAR antibodies were generated by immunizing rabbits (Covance Research Products) with a SPAR peptide corresponding to residues 1323–1335, in which S1328 was phosphorylated. Phospho-antibodies were purified first by negative selection over a column of covalently attached unphosphorylated peptide, followed by binding to a column of phosphorylated peptide. Polyclonal GKBD-SPAR antibodies (used in Figures 5B, 5C, and 6) were generated by immunizing rabbits with purified MBP-GKBD fusion protein.

The polyclonal C-SPAR antibody (used in Figure 5A) has been described (Pak et al., 2001). Mouse monoclonal PSD-95 antibody K28/43 was a gift from J. Trimmer (UC Davis); rabbit polyclonal p25/p35 antibody was a gift from Li-Huei Tsai (MIT). The following antibodies were purchased from commercial sources: mouse monoclonal myc antibody (9E10), myc agarose conjugate, polyclonal GST (Z-5) antibody (Santa Cruz Biotechnology), monoclonal α-tubulin (B-5-1-2) antibody (Sigma), polyclonal GFP antibody (MBL). Aβ(1-40) and Aβ(40-1) (American Peptide Company) were solubilized and used as described (Roselli et al., 2005). Drugs were purchased from Sigma.

Yeast Two-Hybrid and Virus Preparation

Two-hybrid assays were performed using the yeast strain L40 harboring β-gal and HIS3 reporters, as described (Niethammer and Sheng, 1998).

Plk2 was cloned into a modified pSinRep5 vector (Invitrogen) containing GFP preceded by an IRES2 internal ribosomal entry site. Sindbis virus was prepared according to manufacturer guidelines (Invitrogen). Briefly, DNA templates were transcribed using an in vitro transcription kit (Ambion) and then electroporated into BHK cells. 24–36 hr posttransfection, the supernatant was harvested and used for hippocampal culture infection by directly pipetting virus into growth medium. Recordings were performed ~24 hr postinfection under visual guidance of the GFP signal.

HSV packaged with p35 and/or GFP was a gift from Li-Huei Tsai (MIT).

HEK293 Transfection, Doxycycline Time Course, Immunoprecipitation, and GST-"Pull-Downs"

HEK293 cells were transfected using Lipofectamine (Invitrogen). For GST-pull-down and immunoprecipitation assays, cells were lysed in RIPA buffer, and lysates centrifuged at 15,000 × g for 30 min. Myc-antibody (9E10)-coupled agarose, or GST, GST-tagged Plk2-PBD, or GST-tagged Plk2-PBD(W504F) coupled to glutathione Sepharose, were mixed with supernatants for 3 hr at 4°C. After washing five times in RIPA buffer, immunoprecipitates were analyzed by immunoblotting. For doxycycline time course experiments, doxycycline was applied the day after transfection for the indicated times.

Peptide Precipitation Experiments

E. coli (BL21) expressing GST-PBD were lysed by sonication in ice-cold PBS, followed by addition of Triton X-100 (1% final concentration) and shaking at 4°C for 20 min. Lysates were centrifuged at 15,000 × g for 30 min, and supernatants were then incubated with agarose beads coupled to either the phosphorylated pS1328 peptide or the unphosphorylated S1328 peptide for 3 hr at 4°C under gentle agitation. Peptide coupling was performed using the SulfoLink kit (Pierce). After washing in lysis buffer (PBS, 1% TX-100), precipitated protein was analyzed by coomassie staining and immunoblotting.

Dissociated Neuron Culture, Transfection, and Immunostaining

Hippocampal or cortical cultures were prepared and cultured from E19 Sprague Dawley rats as previously described (Pak et al., 2001). Briefly, 150–200 cells mm^{-2} (hippocampal culture) or 1000 cells mm^{-2} (cortical culture) were plated on 19 mm coverslips coated with 30 μg/ml poly-D-lysine and 2 μg/ml laminin. Transfections of hippocampal cultures were performed with Lipofectamine 2000 (Invitrogen) at DIV16–19, and cells were either recorded 3–4 days later or fixed 3 days later in 1% formaldehyde, 4% sucrose in PBS for 2 min at room temperature followed by −20°C MetOH for 10 min for staining of endogenous proteins. Antibodies were applied in GDB buffer (0.1% gelatin, 0.3% TX-100, 450 mM NaCl, 32% 0.1M Phosphate buffer [pH 7.4]).

Electrophysiology

Electrophysiological recordings of hippocampal neurons were performed 3-4 days after transfection in bath solution containing (in mM): 119 NaCl, 2.5 KCl, 2.8 CaCl$_2$, 2 MgCl$_2$, 26 NaHCO$_3$, 1 NaH$_2$PO$_4$, 11 glucose, 0.1 picrotoxin, gassed with 5% CO$_2$/95% O$_2$ at pH 7.4. Recordings were carried out at 30-34°C. TTX (1 μM) was added to block action potentials. Whole-cell recordings were made under visual guidance with the aid of IR-DIC optics. Cells were recorded from for roughly 5 min to obtain at least 100 events/cell.

Pipettes (2.5–4 MΩ) were filled with an internal solution containing (in mM): 115 cesium methanesulfonate, 20 CsCl, 10 HEPES, 2. 5 MgCl$_2$, 4 ATP disodium salt, 0.4 GTP trisodium salt, 10 sodium phosphocreatine, and 0.6 EGTA, at pH 7.25.

Whole-cell voltage-clamp recordings were made using a Multiclamp 700A amplifier (Axon Instruments). Current signals were filtered at 2 kHz and digitized at 10 kHz with a Digidata 1322A (Axon Instruments). Analysis of recordings was performed using Clampfit software (Axon Instruments). Recordings and quantitation were performed blind to experimental conditions.

Imaging and Quantitation

Images were acquired using an LSM510 confocal system with an oil-immersion 63X objective (NA 1.4, Zeiss). Confocal Z-series image stacks encompassing entire dendrite segments were analyzed using MetaMorph software (Universal Imaging Corporation). For measurements of SPAR immunofluorescence intensity as a function of distance from the soma, concentric circles increasing in 10 μm steps were traced around the soma, and three to four dendritic segments of 90 μm were analyzed from thresholded images. For each condition, integrated SPAR immunofluorescence intensity levels from distinct dendrites for each distance (i.e., dendritic segments bound by the same two circles) were first grouped and averaged per neuron. Means from several neurons were then averaged to obtain a population mean and normalized to the 10 μm population mean in vehicle-treated controls (presented as mean ± SEM). SPAR immunofluorescence intensity levels from transfected cells are from thresholded images and represent integrated intensity measurements per unit length of dendrite. SPAR immunofluorescence intensity levels from three to four dendritic segments of 90 μm were collected and averaged per neuron. Average SPAR immunofluorescence intensities for each transfected cell were normalized to values obtained from nearby untransfected cells and then averaged with cells transfected with the same construct to obtain a population mean (presented as mean ± SEM). All imaging and quantitation were performed blind to experimental conditions.

Statistical Analysis

Statistical Methods are described in the Figure Legends.

SUPPLEMENTAL DATA

The Supplemental Data for this article, which include a table and figures, can be found online at http://www.neuron.org/cgi/content/full/58/4/571/DC1/.

ACKNOWLEDGMENTS

REFERENCES

Alvarez, A., Munoz, J.P., and Maccioni, R.B. (2001). A Cdk5-p35 stable complex is involved in the beta-amyloid-induced deregulation of Cdk5 activity in hippocampal neurons. Exp. Cell Res. *264*, 266–274.

Brummelkamp, T.R., Bernards, R., and Agami, R. (2002). A system for stable expression of short interfering RNAs in mammalian cells. Science *296*, 550–553.

Bui, C.J., McGann, A.C., Middleton, F.A., Beaman-Hall, C.M., and Vallano, M.L. (2006). Transcriptional profiling of depolarization-dependent phenotypic alterations in primary cultures of developing granule neurons. Brain Res. *1119*, 13–25.

Burgoyne, R.D., O'Callaghan, D.W., Hasdemir, B., Haynes, L.P., and Tepikin, A.V. (2004). Neuronal Ca2+-sensor proteins: multitalented regulators of neuronal function. Trends Neurosci. *27*, 203–209.

Burrone, J., and Murthy, V.N. (2003). Synaptic gain control and homeostasis. Curr. Opin. Neurobiol. *13*, 560–567.

Davis, G.W. (2006). Homeostatic control of neural activity: from phenomenology to molecular design. Annu. Rev. Neurosci. *29*, 307–323.

Elia, A.E., Cantley, L.C., and Yaffe, M.B. (2003a). Proteomic screen finds pSer/pThr-binding domain localizing Plk1 to mitotic substrates. Science *299*, 1228–1231.

Elia, A.E., Rellos, P., Haire, L.F., Chao, J.W., Ivins, F.J., Hoepker, K., Mohammad, D., Cantley, L.C., Smerdon, S.J., and Yaffe, M.B. (2003b). The molecular basis for phosphodependent substrate targeting and regulation of Plks by the Polo-box domain. Cell *115*, 83–95.

Fabbro, M., Zhou, B.B., Takahashi, M., Sarcevic, B., Lal, P., Graham, M.E., Gabrielli, B.G., Robinson, P.J., Nigg, E.A., Ono, Y., and Khanna, K.K. (2005). Cdk1/Erk2- and Plk1-dependent phosphorylation of a centrosome protein, Cep55, is required for its recruitment to midbody and cytokinesis. Dev. Cell *9*, 477–488.

Fu, Z., Lee, S.H., Simonetta, A., Hansen, J., Sheng, M., and Pak, D.T. (2007). Differential roles of Rap1 and Rap2 small GTPases in neurite retraction and synapse elimination in hippocampal spiny neurons. J. Neurochem. *100*, 118–131.

Goddard, C.A., Butts, D.A., and Shatz, C.J. (2007). Regulation of CNS synapses by neuronal MHC class I. Proc. Natl. Acad. Sci. USA *104*, 6828–6833.

Goldberg, J.H., and Yuste, R. (2005). Space matters: local and global dendritic Ca2+ compartmentalization in cortical interneurons. Trends Neurosci. *28*, 158–167.

Gong, B., Wang, H., Gu, S., Heximer, S.P., and Zhuo, M. (2007). Genetic evidence for the requirement of adenylyl cyclase 1 in synaptic scaling of forebrain cortical neurons. Eur. J. Neurosci. *26*, 275–288.

Gonzalez-Islas, C., and Wenner, P. (2006). Spontaneous network activity in the embryonic spinal cord regulates AMPAergic and GABAergic synaptic strength. Neuron *49*, 563–575.

Guan, Z., Saraswati, S., Adolfsen, B., and Littleton, J.T. (2005). Genome-wide transcriptional changes associated with enhanced activity in the Drosophila nervous system. Neuron *48*, 91–107.

Hevroni, D., Rattner, A., Bundman, M., Lederfein, D., Gabarah, A., Mangelus, M., Silverman, M.A., Kedar, H., Naor, C., Kornuc, M., et al. (1998). Hippocampal plasticity involves extensive gene induction and multiple cellular mechanisms. J. Mol. Neurosci. *10*, 75–98.

Hosokawa, T., Saito, T., Asada, A., Ohshima, T., Itakura, M., Takahashi, M., Fukunaga, K., and Hisanaga, S. (2006). Enhanced activation of Ca2+/calmodulin-dependent protein kinase II upon downregulation of cyclin-dependent kinase 5-p35. J. Neurosci. Res. *84*, 747–754.

Hou, Q., Zhang, D., Jarzylo, L., Huganir, R.L., and Man, H.Y. (2008). Homeostatic regulation of AMPA receptor expression at single hippocampal synapses. Proc. Natl. Acad. Sci. USA *105*, 775–780.

Hsieh, H., Boehm, J., Sato, C., Iwatsubo, T., Tomita, T., Sisodia, S., and Malinow, R. (2006). AMPAR removal underlies Abeta-induced synaptic depression and dendritic spine loss. Neuron *52*, 831–843.

Huang, C.C., You, J.L., Wu, M.Y., and Hsu, K.S. (2004). Rap1-induced p38 mitogen-activated protein kinase activation facilitates AMPA receptor trafficking via the GDI.Rab5 complex. Potential role in (S)-3,5-dihydroxyphenylglycene-induced long term depression. J. Biol. Chem. *279*, 12286–12292.

Jiang, N., Wang, X., Jhanwar-Uniyal, M., Darzynkiewicz, Z., and Dai, W. (2006). Polo box domain of Plk3 functions as a centrosome localization signal, overexpression of which causes mitotic arrest, cytokinesis defects, and apoptosis. J. Biol. Chem. *281*, 10577–10582.

Ju, W., Morishita, W., Tsui, J., Gaietta, G., Deerinck, T.J., Adams, S.R., Garner, C.C., Tsien, R.Y., Ellisman, M.H., and Malenka, R.C. (2004). Activity-dependent regulation of dendritic synthesis and trafficking of AMPA receptors. Nat. Neurosci. *7*, 244–253.

Kamenetz, F., Tomita, T., Hsieh, H., Seabrook, G., Borchelt, D., Iwatsubo, T., Sisodia, S., and Malinow, R. (2003). APP processing and synaptic function. Neuron *37*, 925–937.

Kauselmann, G., Weiler, M., Wulff, P., Jessberger, S., Konietzko, U., Scafidi, J., Staubli, U., Bereiter-Hahn, J., Strebhardt, K., and Kuhl, D. (1999). The polo-like protein kinases Fnk and Snk associate with a Ca(2+)- and integrin-binding protein and are regulated dynamically with synaptic plasticity. EMBO J. *18*, 5528–5539.

Kim, E., Niethammer, M., Rothschild, A., Jan, Y.N., and Sheng, M. (1995). Clustering of Shaker-type K+ channels by interaction with a family of membrane-associated guanylate kinases. Nature *378*, 85–88.

Lee, M.S., Kwon, Y.T., Li, M., Peng, J., Friedlander, R.M., and Tsai, L.H. (2000). Neurotoxicity induces cleavage of p35 to p25 by calpain. Nature *405*, 360–364.

Lowery, D.W., Mohammad, D.H., Elia, A.E., and Yaffe, M.B. (2004). The Polo-box domain: a molecular integrator of mitotic kinase cascades and Polo-like kinase function. Cell Cycle *3*, 128–131.

Ma, S., Charron, J., and Erikson, R.L. (2003a). Role of Plk2 (Snk) in mouse development and cell proliferation. Mol. Cell. Biol. *23*, 6936–6943.

Ma, S., Liu, M.A., Yuan, Y.L., and Erikson, R.L. (2003b). The serum-inducible protein kinase Snk is a G(1) phase Polo-like kinase that is inhibited by the calcium- and integrin-binding protein CIB. Mol. Cancer Res. *1*, 376–384.

Majdan, M., and Shatz, C.J. (2006). Effects of visual experience on activity-dependent gene regulation in cortex. Nat. Neurosci. *9*, 650–659.

Mattson, M.P. (2004). Pathways towards and away from Alzheimer's disease. Nature *430*, 631–639.

Meijer, L., Borgne, A., Mulner, O., Chong, J.P., Blow, J.J., Inagaki, N., Inagaki, M., Delcros, J.G., and Moulinoux, J.P. (1997). Biochemical and cellular effects of roscovitine, a potent and selective inhibitor of the cyclin-dependent kinases cdc2, cdk2 and cdk5. Eur. J. Biochem. *243*, 527–536.

Nedivi, E., Hevroni, D., Naot, D., Israeli, D., and Citri, Y. (1993). Numerous candidate plasticity-related genes revealed by differential cDNA cloning. Nature *363*, 718–722.

Niethammer, M., and Sheng, M. (1998). Identification of ion channel-associated proteins using the yeast two-hybrid system. Methods Enzymol. *293*, 104–122.

Nikolic, M., Dudek, H., Kwon, Y.T., Ramos, Y.F., and Tsai, L.H. (1996). The cdk5/p35 kinase is essential for neurite outgrowth during neuronal differentiation. Genes Dev. *10*, 816–825.

Obenauer, J.C., Cantley, L.C., and Yaffe, M.B. (2003). Scansite 2.0: Proteome-wide prediction of cell signaling interactions using short sequence motifs. Nucleic Acids Res. *31*, 3635–3641.

Pak, D.T., and Sheng, M. (2003). Targeted protein degradation and synapse remodeling by an inducible protein kinase. Science *302*, 1368–1373.

Pak, D.T., Yang, S., Rudolph-Correia, S., Kim, E., and Sheng, M. (2001). Regulation of dendritic spine morphology by SPAR, a PSD-95-associated RapGAP. Neuron *31*, 289–303.

Qi, W., Tang, Z., and Yu, H. (2006). Phosphorylation- and polo-box-dependent binding of Plk1 to Bub1 is required for the kinetochore localization of Plk1. Mol. Biol. Cell *17*, 3705–3716.

Qian, Z., Gilbert, M.E., Colicos, M.A., Kandel, E.R., and Kuhl, D. (1993). Tissue-plasminogen activator is induced as an immediate-early gene during seizure, kindling and long-term potentiation. Nature *361*, 453–457.

Roselli, F., Tirard, M., Lu, J., Hutzler, P., Lamberti, P., Livrea, P., Morabito, M., and Almeida, O.F. (2005). Soluble beta-amyloid1-40 induces NMDA-dependent degradation of postsynaptic density-95 at glutamatergic synapses. J. Neurosci. *25*, 11061–11070.

Ross, W.N. (1989). Changes in intracellular calcium during neuron activity. Annu. Rev. Physiol. *51*, 491–506.

Rutherford, L.C., Nelson, S.B., and Turrigiano, G.G. (1998). BDNF has opposite effects on the quantal amplitude of pyramidal neuron and interneuron excitatory synapses. Neuron *21*, 521–530.

Seong, Y.S., Kamijo, K., Lee, J.S., Fernandez, E., Kuriyama, R., Miki, T., and Lee, K.S. (2002). A spindle checkpoint arrest and a cytokinesis failure by the dominant-negative polo-box domain of Plk1 in U-2 OS cells. J. Biol. Chem. *277*, 32282–32293.

Shepherd, J.D., Rumbaugh, G., Wu, J., Chowdhury, S., Plath, N., Kuhl, D., Huganir, R.L., and Worley, P.F. (2006). Arc/Arg3.1 mediates homeostatic synaptic scaling of AMPA receptors. Neuron *52*, 475–484.

Simmons, D.L., Neel, B.G., Stevens, R., Evett, G., and Erikson, R.L. (1992). Identification of an early-growth-response gene encoding a novel putative protein kinase. Mol. Cell. Biol. *12*, 4164–4169.

Stellwagen, D., and Malenka, R.C. (2006). Synaptic scaling mediated by glial TNF-alpha. Nature *440*, 1054–1059.

Sutton, M.A., Ito, H.T., Cressy, P., Kempf, C., Woo, J.C., and Schuman, E.M. (2006). Miniature neurotransmission stabilizes synaptic function via tonic suppression of local dendritic protein synthesis. Cell *125*, 785–799.

Thiagarajan, T.C., Piedras-Renteria, E.S., and Tsien, R.W. (2002). alpha- and betaCaMKII. Inverse regulation by neuronal activity and opposing effects on synaptic strength. Neuron *36*, 1103–1114.

Thiagarajan, T.C., Lindskog, M., Malgaroli, A., and Tsien, R.W. (2006). LTP and adaptation to inactivity: Overlapping mechanisms and implications for metaplasticity. Neuropharmacology *52*, 156–175.

Town, T., Zolton, J., Shaffner, R., Schnell, B., Crescentini, R., Wu, Y., Zeng, J., DelleDonne, A., Obregon, D., Tan, J., and Mullan, M. (2002). p35/Cdk5 pathway mediates soluble amyloid-beta peptide-induced tau phosphorylation in vitro. J. Neurosci. Res. *69*, 362–372.

Tropea, D., Kreiman, G., Lyckman, A., Mukherjee, S., Yu, H., Horng, S., and Sur, M. (2006). Gene expression changes and molecular pathways mediating activity-dependent plasticity in visual cortex. Nat. Neurosci. *9*, 660–668.

Turrigiano, G. (2007). Homeostatic signaling: the positive side of negative feedback. Curr. Opin. Neurobiol. *17*, 318–324.

Turrigiano, G.G., Leslie, K.R., Desai, N.S., Rutherford, L.C., and Nelson, S.B. (1998). Activity-dependent scaling of quantal amplitude in neocortical neurons. Nature *391*, 892–896.

van de Weerdt, B.C., and Medema, R.H. (2006). Polo-like kinases: a team in control of the division. Cell Cycle *5*, 853–864.

Walsh, D.M., and Selkoe, D.J. (2004). Deciphering the molecular basis of memory failure in Alzheimer's disease. Neuron *44*, 181–193.

Wei, F.Y., Tomizawa, K., Ohshima, T., Asada, A., Saito, T., Nguyen, C., Bibb, J.A., Ishiguro, K., Kulkarni, A.B., Pant, H.C., et al. (2005). Control of cyclin-dependent kinase 5 (Cdk5) activity by glutamatergic regulation of p35 stability. J. Neurochem. *93*, 502–512.

Wyszynski, M., Lin, J., Rao, A., Nigh, E., Beggs, A.H., Craig, A.M., and Sheng, M. (1997). Competitive binding of alpha-actinin and calmodulin to the NMDA receptor. Nature *385*, 439–442.

Xie, Z., Huganir, R.L., and Penzes, P. (2005). Activity-dependent dendritic spine structural plasticity is regulated by small GTPase Rap1 and its target AF-6. Neuron *48*, 605–618.

Yamagata, K., Andreasson, K.I., Kaufmann, W.E., Barnes, C.A., and Worley, P.F. (1993). Expression of a mitogen-inducible cyclooxygenase in brain neurons: regulation by synaptic activity and glucocorticoids. Neuron *11*, 371–386.

Zhu, J.J., Qin, Y., Zhao, M., Van Aelst, L., and Malinow, R. (2002). Ras and Rap control AMPA receptor trafficking during synaptic plasticity. Cell *110*, 443–455.

Zhu, Y., Pak, D., Qin, Y., McCormack, S.G., Kim, M.J., Baumgart, J.P., Velamoor, V., Auberson, Y.P., Osten, P., van Aelst, L., et al. (2005). Rap2-JNK removes synaptic AMPA receptors during depotentiation. Neuron *46*, 905–916.